NJC

Accepted Manuscript

This is an *Accepted Manuscript*, which has been through the Royal Society of Chemistry peer review process and has been accepted for publication.

Accepted Manuscripts are published online shortly after acceptance, before technical editing, formatting and proof reading. Using this free service, authors can make their results available to the community, in citable form, before we publish the edited article. We will replace this *Accepted Manuscript* with the edited and formatted *Advance Article* as soon as it is available.

You can find more information about *Accepted Manuscripts* in the Information for Authors.

Please note that technical editing may introduce minor changes to the text and/or graphics, which may alter content. The journal's standard Terms & Conditions and the Ethical guidelines still apply. In no event shall the Royal Society of Chemistry be held responsible for any errors or omissions in this *Accepted Manuscript* or any consequences arising from the use of any information it contains.

ROYAL SOCIETY OF CHEMISTRY

www.rsc.org/njc

Synthesis and Antimicrobial Activity of Aminoglycoside-Conjugated Silica Nanoparticles on Clinical and Resistant Bacteria

Shrish Agnihotri,[a,c] Rajiv Pathak,[b] Diksha Jha,[b] Indrajit Roy,[c] Hemant K. Gautam,[b] Ashwani K. Sharma[a] and Pradeep Kumar*[a]

[a] Nucleic Acids Research laboratory, CSIR-Institute of Genomics and Integrative Biology, Mall Road, Delhi-110007, India
[b] Microbial Biotechnology Laboratory, CSIR-Institute of Genomics and Integrative Biology, Sukhdev Vihar, Mathura Road, New Delhi-110025, India
[c] Department of Chemistry, University of Delhi, Delhi-110007, India

***Address for correspondence**
Dr. Pradeep Kumar
Nucleic Acids Research laboratory,
CSIR-Institute of Genomics and Integrative Biology,
Mall Road, Delhi-110007, India
Fax: +91 11 27667471
Tel: +91 11 27662491
E-mail: pkumar@igib.res.in

KEYWORDS: Silica nanoparticles, aminoglycosides, antimicrobial activity, hemolysis and cell viability, drug resistance.

Abstract

Functionalization of silica nanoparticles with different cationic moieties make them suitable for being an effective antimicrobial agent against various clinical pathogenic microbes. Here, we report synthesis, characterization and evaluation of aminoglycoside-conjugated silica nanoparticles [S-X NPs, where X= Gentamicin (G), Neomycin (N) or Kanamycin (K)] for their antimicrobial activity against clinical pathogens and kanamycin-resistant *E. coli*. These functionalized silica nanoparticles exhibited enhanced broad-spectrum antimicrobial activity against clinical Gram-positive and Gram-negative bacteria as well as kanamycin-resistant *E. coli* strain with minimal cytotoxicity. The results show potential of these conjugates to combat drug resistance.

Introduction

Microorganisms are the major cause of infections and infection-derived fatal diseases. The majority of these are hospital-acquired infections, which have accounted for a significant number of deaths annually worldwide.[1-3] Inapt use of antibiotics as well as lack of new antibiotics in the pipeline has further worsened the global human healthcare systems leading to the development of resistant strains of bacteria[4,5] that has resulted in the ineffectiveness of a large number of currently available antibacterials. To address this challenge, sincere efforts have been made to develop alternative strategies and antimicrobial therapeutics based on natural- or synthetic compounds having different mode of action.[5] Recently, these agents have also emerged as the important class of compounds which are finding extentive use in the areas such as food packaging,[6,7] sterilized devices,[8] cosmetics,[9] leather preservation,[10,11] etc. These are mostly derived from both natural as well as synthetic polymers alone or consisting of active compounds such as silver, triclosan, sulphur dioxide, chlorine dioxide, essential oils etc. Mechanistically, most of the antimicrobials kill microorganisms in two ways,[12] viz., (i) diffusion killing, and (ii) contact killing. In the foremost one, antimicrobial agents of low molecular weight diffuse inside the cells and bind to some key compounds of bacterial metabolism affecting the normal cellular activities followed by killing. In the later one, the antimicrobials kill bacteria immediately on contact by causing the bacterial cell to burst.[13] Most of the cationic polymer-based antimicrobials kill bacteria through this method by adsorbing onto negatively charged bacterial surfaces. Besides possessing antimicrobial activity, these polymers have also shown some degree of selectivity against the bacterial membranes i.e. they are toxic to microbes but non-toxic to human cells. Hence, these are considered as potential future therapeutic agents. Low molecular weight antimicrobials are efficient, but repeated uses lead to the development of resistance, their activity is for short duration and moreover, they impart toxicity due to their ability to permeate through human and animal skin.[14] Therefore, polymer-based antimicrobials are preferred due to their long lifetime, eco-safety, low cytotoxicity, low volatility and the inability to induce bacterial resistance. [15-17] Some of the commonly used polymers and their analogs for this purpose are polyquaterniums, polyphosphoniums, polyethylenimines, polyallylamine, dendrimers, etc.[17-20]

Recently, silica nanoparticles have been shown to act as an efficient carrier of biomolecules[21-23] and attracted the attention of researchers as they possess high stability and durability, and easily modified by established organosilane chemistry, allowing the incorporation

of an array of functional groups. The large surface area of silica nanoparticles along with high chemical, thermal and colloidal stability as well as easy functionalization have made it suitable for use as a biochemical agent.[24,25] Surface-functionalized silica nanomaterials can easily penetrate animal and plant cells without causing any significant cytotoxicity issue *in vitro*.[26-28] Not many studies have been carried out using such conjugates. Hence, these developments render the possibility of designing a new generation of antimicrobial agents based on polyamines for the treatment of a wide range of intracellular pathogens including resistant strains.[29-32]

Herein, we report the functionalization of silica nanoparticles with broad spectrum aminoglycosides (Gentamicin, G; Neomycin, N; Kanamycin, K) using an epoxy-amine chemistry.[33] Aminoglycosides consist of essential six-membered rings with various types of amines. They display excellent activity against gram-negative bacteria, however, are not preferred for gram-positive bacteria due to their lack of activity.[34-36] Subsequently, these aminoglycoside-conjugated silica nanoparticles were subjected to physicochemical characterization followed by evaluation for their antimicrobial activity on gram-positive (*Bacillus cereus, BC* and *Staphylococcus aureus, SA*) and gram-negative (*Escherichia coli, EC* and *Salmonella enteric typhimurium, ST*) bacteria as well as kanamycin-resistant *E. coli.* Further, the usefulness of the projected nanoparticles was demonstrated by performing cytotoxicity assays on hRBCs and mammalian cells. The results showed that aminoglycoside-conjugated silica nanoparticles possessed excellent antimicrobial activity against both the strains and kanamycin-conjugated silica nanoparticles were found to be highly efficient against kanamycin-resistant *E. coli*. Apart from these, these nanoparticles showed excellent blood compatibility and low toxicity.

Experimental

Materials

3-Glycidyloxypropyltrimethoxysilane, aminoglycosides (gentamicin sulphate, neomycin trisulfate and kanamycin sulphate) and iodonitrotetrazolium chloride (INT), MTT [3-(4,5-dimethylthiazol-2-yl)-2,5-diphenyltetrazolium bromide] were purchased from Sigma-Aldrich Chemical Company, USA. Silica nanoparticles (20-30 nm) were procured from J. K. Impex, Mumbai, India. All other reagents and chemicals used in the present study were obtained from local vendors and purified prior to their use. Milli Q water filtered through 0.22 μm membrane filter was used in all experiments.

Synthesis and characterization of aminoglycoside-conjugated silica nanoparticles

(a) Synthesis of functionalized silica nanoparticles

Functionalized silica nanoparticles (aminoglycoside-conjugated silica nanoparticles) were prepared in a two-step process. In the first step, silica nanoparticles (1.0 g) were suspended in a 10% solution of 3-glycidyloxypropyltrimethoxysilane in anhydrous toluene (50 ml) and kept at 60 ^{o}C for 48h with occasional shaking. Then the solution was transferred to centrifuge tubes and

centrifuged at 9000 rpm for 15 min. The solvent was decanted off and the particles were washed with dry toluene (5 x 50 ml) followed by diethylether (2 x 50 ml) following the centrifugation procedure and dried. In the subsequent step, a solution of an aminoglycoside (gentamicin sulphate, 200 mg), dissolved in water (5 ml) and triethylamine (0.5 ml), was added to activated silica nanoparticles (epoxy group bearing nanoparticles) (200 mg) suspended in isopropanol (2 ml) and the suspension was placed at 60 ^{o}C for 24h in an incubator shaker. Then isopropanol:water (1:1, 20 ml, v/v) was added and the resulting suspension was centrifuged. The supernatant was taken away and the particles were further washed sequentially with isopropanol: water (1:1, v/v, 3 x 25 ml), methanol (2 x 25 ml) and diethylether (2 x 25 ml). Finally, these particles were dried in a vacuum desiccator to obtain gentamicin-conjugated silica nanoparticles (S-G NPs). Likewise, neomycin- and kanamycin-conjugated silica nanoparticles (S-N and S-K NPs) were prepared and dried. These functionalized silica nanoparticles were then characterized by Fourier Transform Infrared (FTIR) spectroscopy, thermogravimetric analysis (TGA), X-ray diffraction (XRD), dynamic light scattering (DLS) and transmission electron microscopy (TEM).

(b) Characterization

(i) Size and zeta potential measurements

Aqueous solutions of native silica nanoparticles and aminoglycoside-conjugated silica nanoparticles (1 mg/ml) were used for DLS measurement using Zetasizer Nano-ZS (Malvern Inc., UK). Samples prepared for the DLS measurement were sonicated (Power 500 W, Amplitude 30%, Reaction time = 50 min, pulse on: 30s and pulse off: 30s in an ice-bath) well before measurement due to the large aggregation. Size and zeta potential measurements were carried out in triplicate in automatic mode for an average of 20 and 30 runs, respectively.

(ii) FTIR spectroscopy

FTIR spectra of the functionalized silica nanoparticles (~2 mg) were recorded on a single beam Perkin Elmer (Spectrum RXI-MID IR), USA, with the following scan parameters: scan range, 4400–400 cm^{-1}; number of scans, 16; resolution, 4.0 cm^{-1}; interval, 1.0 cm^{-1}; unit %T.

(iii) X-ray Diffraction (XRD) analysis

Powdered samples containing silica nanoparticles and functionalized silica nanoparticles were subjected to X-ray diffraction measurements on X'pert PRO XRD, Analytical BV, Almelo, Netherlands, operating in transmission mode at 30 kV, 20 mA with Cu-Ka radiation.

(iv) Thermogravimetric analysis (TGA)

Thermogravimetric analysis (TGA) of native and functionalized silica nanoparticles (~4 mg) was carried out on Perkin Elmer Pyris Diamond TGA (USA) equipped with TG units at a heating rate of 10 ^{o}C/min from 30 ^{o}C to 900 ^{o}C under nitrogen atmosphere. A graph between temperature (^{o}C) and subtracted mass (percent weight loss) was plotted.

(v) Transmission electron microscopy (TEM)

For electron microscopy, 2 μl of nanoparticle solution (1 mg/ml) was deposited on carbon-coated grid and added a solution of 1% uranyl acetate for 2-3 min. The grids were air-dried and subjected to imaging under transmission electron microscopy. The images were captured at an accelerating voltage of 200kV (Tecnai G2 30U-twin, Tecnai 300kV ultratwin microscope).

Biological Activities

(a) Microorganisms and growth conditions

Bacillus cereus (B. cereus) (MTCC 430), *Staphylococcus aureus (S. aureus)* (MTCC 740) *Escherichia coli (E. coli)* (MTCC 1586) and *Salmonella enteric typhimurium (S. typhimurium)* (MTCC 98) were grown at 37 ^{o}C in Mueller Hinton broth prior to use. The microorganisms were stored in brain heart infusion broth supplemented with 40% glycerol at -70º C.

(b) Interaction studies of functionalized silica nanoparticles with bacterial cells using TEM

Interaction of aminoglycoside-conjugated silica nanoparticles with bacterial cells was investigated by TEM. Functionalized silica nanoparticles (1 mg/ml) were incubated with freshly prepared culture of *B. cereus* at different time points (15, 30 and 60 min) at 37 ^{o}C. After stipulated time periods, the culture was centrifuged and the pellet was thoroughly washed with 1x PBS (3 x1 ml). Then each of the bacterial cell pellet, thus obtained after centrifugation, was fixed with a 4% solution of paraformaldehyde and the pellet was kept at 4˚C for overnight. After centrifugation, each pellet was washed again with 1x PBS (3 x 1ml). Finally, sequential dehydration of bacterial cells was carried out by washing with solutions of increasing concentrations of ethanol (e.g. 10%, 20%, 40%, 60%, 80% and 100%). The pellet was again suspended in 1x PBS and deposited on the TEM grids as described above using 1% uranyl acetate as a staining reagent.

(c) Microbroth dilution assay

The Microbroth dilution assay was performed in sterile 96-well plates with cover (Nunc, Corning). Sterile glass tubes having freshly autoclaved media (Mueller Hinton Broth) dissolved in MilliQ water (Millipore) was used for culturing the microbes. Different concentrations of the samples were made in autoclaved MilliQ water pH 7.2, filtered through 0.22 μm sterile filters (Millipore, USA). Corresponding aminoglycoside and autoclaved MilliQ water were kept as positive and negative controls, respectively. Iodonitrotetrazolium chloride (INT) was used as a growth indicator. The entire procedure was performed in a sterile Laminar Hood and the microbes were incubated in a shaker incubator operating at 37º C.

Three concentrations of aminoglycoside-conjugated silica nanoparticles (1 mg/ml, 2 mg/ml and 4 mg/ml) were made in Mueller Hinton Broth and inoculated with 30μl of 1 x 10^5 CFU/ml fresh cultures of *B. cereus, S. aureus, E. coli* and *S. typhimurium* in a 96-well plate. The

volume was made up to 250µl with fresh Mueller Hinton Broth. Following overnight incubation at 37˚C, wells of the plates were examined for visible bacterial growth. Optical density (O.D.) was taken at 600 nm at different time intervals of 0, 3, 6, 9, 12 and 15 h. Then to ascertain the antibacterial activity of the silica samples (native and functionalized), *p*-iodonitrotetrazolium chloride (INT) dye solution (0.25 mg/ml) was used as an indicator to actually visualize the bacterial growth colorimetrically. 30µl of the dye solution (INT) was added to each well and kept the plate in a rotary shaker incubator at 37˚C for 30 min. The appearance of pink to red color indicated bacterial growth and the wells which remained colorless showed the antibacterial activity. Graphs between the bacterial growth (OD_{600}) with native silica and functionalized silica nanoparticles were plotted as a function of time (h).

(d) Minimum inhibitory concentration (MIC)

It is the lowest concentration of the antibacterial agent to completely inhibit the growth of the bacterial cultures. In order to determine the MIC of aminoglycoside-conjugated silica nanoparticles (S-G, S-N and S-K NPs), a range of serially diluted samples were prepared. The dilution was restructured according to the results obtained by the microbroth dilution method. After careful adjustments, following dilutions were prepared, viz., 600, 400, 300, 200, 100, 95, 90, 85, 80, 75, 70, 65, 60 µg/ml. Concentrations of native silica nanoparticles were made at 10, 20 and 30 mg/ml. For S-K NPs, the assay was repeated at 440, 420, 400, 380, 360, 340, 320, 300 µg/ml. The protocol to determine antimicrobial activity remained same as that was followed in microbroth dilution method. The experiment was conducted in triplicates to check the reproducibility of the results.

(e) Antibacterial activity against kanamycin-resistant *E. coli*

Kanamycin-resistant *E. coli* (CGSC 11903) was cultured in LB broth and incubated at 37 ^{o}C so as to attain optical density of 0.6. A solution of S-K nanoparticles was sonicated as described above to get a homogeneous solution. Then in a 96-well plate, MHB media was put according to the calculation for 1x, 5x, 10x MIC values of the S-K NPs found against *E. coli.* 10 µl of the resistant *E. coli* strain was poured in each well with the exact volume of S-K NPs for 1x, 5x, 10x MIC values. Same protocol was followed with the standard kanamycin antibiotic and the concentration was taken according to 1x, 5x and 10x of its own MIC value. The plate was incubated at 37 ^{o}C on a shaker incubator for 12h. Optical density was measured at 0, 3, 6 and 9 h of incubation at 600nm using TECAN microplate reader to determine the survival percentage of the bacteria. After 12h of incubation, 30 µl iodonitrotetrazolium chloride (INT, 0.25 mg/ml) dye was added to each well and subjected to colorimetric estimation.

Cytotoxicity Evaluation

(a) Cell viability assay

Cell viability assay of aminoglycosides-conjugated silica nanoparticles was performed in eukaryotic mammalian cell line, MCF-7 (breast cancer cells). The cells were seeded at $6x10^3$ cells per well in 96-well plates and incubated for 36 h. After attaining ~70% confluency, the media was removed and the cells were washed with 1x PBS. Solutions of functionalized silica nanoparticles (S-G, S-N, S-K) and aminoglycosides (G, N and K) were prepared at different concentrations, viz., 1x, 5x and 10x of their MICs in complete media. Similarly, solution of native silica nanoparticles (Si-NPs) was prepared at 10x (4.0 mg/ml) concentration. These solutions were added onto the cells seeded in 96-well plates and incubated for 48 h in humidified 5% CO_2 atmosphere. After incubation, 100 µl of MTT solution (1 mg/ml in serum free media) was added to each well and again the cells were incubated for 2 h. The formazan cystals thus formed were solubilized in 100 µl of DMSO. The plate was centrifuged for 15 min at 4000 rpm and the supernatant was transferred to another plate. The untreated cells were taken as control. The intensity of color was measured spectrophotometrically at 540 nm on an ELISA plate reader. The relative cell survival percentage compared to control was calculated by using the formula:

$$\textbf{Relative cell viability (\%)} = (A_{sample}/A_{control}) \textbf{ X 100}$$

(b) Hemolytic activity

Hemolytic activity of functionalized silica nanoparticles was determined on human erythrocytes also called human Red blood cells (RBCs). The concentrated human RBCs were washed with 1x phosphate buffered saline (PBS, pH 7.4) and suspended in PBS. Different concentrations of functionalized silica nanoparticles from 1 to 50x of their MIC values were taken and diluted with PBS to make final solution 100 µl and then 100 µl of diluted RBCs solution in 1x PBS was mixed in a 96-well plate. The plate was incubated at 37 ºC for 1h and then centrifuged at 800g for 5 min. The supernatant was collected in another 96-well plate and absorbance was taken at 540nm using TECAN microplate reader. The absorbance of RBCs treated with Triton X-100 was used as 100% hemolysis and taken as positive control. 1x PBS was used as negative control. Percent hemolysis was calculated by using the following formula and plotted percent hemolysis vs. concentration (µg/ml).

$$\textbf{Percent hemolysis} = A_{sample}/A_{Triton\text{-}X} \times 100$$

Results and Discussion

Synthesis and characterization of aminoglycoside-conjugated silica nanoparticles

Synthetic steps to prepare aminoglycoside-conjugated silica nanoparticles are depicted in Scheme 1. Epoxy groups were generated on the silica nanoparticles following the standard silanization chemistry using 3-glycidyloxypropyltrimethoxysilane (GOPTS).[37] Subsequent functionalization with three aminoglycosides, G, N and K under basic conditions, generated three different functionalized silica nanoparticles, S-G, S-N and S-K NPs. Extensive washings with different solvents followed by ninhydrin test confirmed the covalent linkage formed between aminoglycoside and epoxy-silica nanoparticles. The particles were found to disperse completely in aqueous solutions upon sonication. Solutions of all the three conjugates (1mg/ml) were sonicated and subjected to Dynamic Light Scattering (DLS) analysis. Native silica nanoparticles showed the average size of ~160 nm, while epoxy-silica (Si-ep) nanoparticles displayed an increase in the size of the particles to ~223 nm indicating activation of silica nanoparticles with epoxy groups. After reaction with different aminoglycosides, fully functionalized silica nanoparticles showed a further increase in the size of the nanoparticles, i.e. size of S-G nanoparticles, ~256 nm; S-N nanoparticles, ~298 nm; S-K nanoparticles, ~269 nm (Table 1). Similarly, the zeta potential measurements showed that silica nanoparticles were strongly negatively charged (~ -41 mV), while epoxy-derivatized silica nanoparticles (Si-ep NPs) showed surface charge of ~ -31 mV. Conjugation of aminoglycosides to epoxy-silica nanoparticles reversed the polarity on the so formed functionalized silica NPs and zeta potential measurements yielded charge on S-G, ~ +34 mV; S-N, ~ +35.5 mV and S-K ~ +24 mV (Table 1).

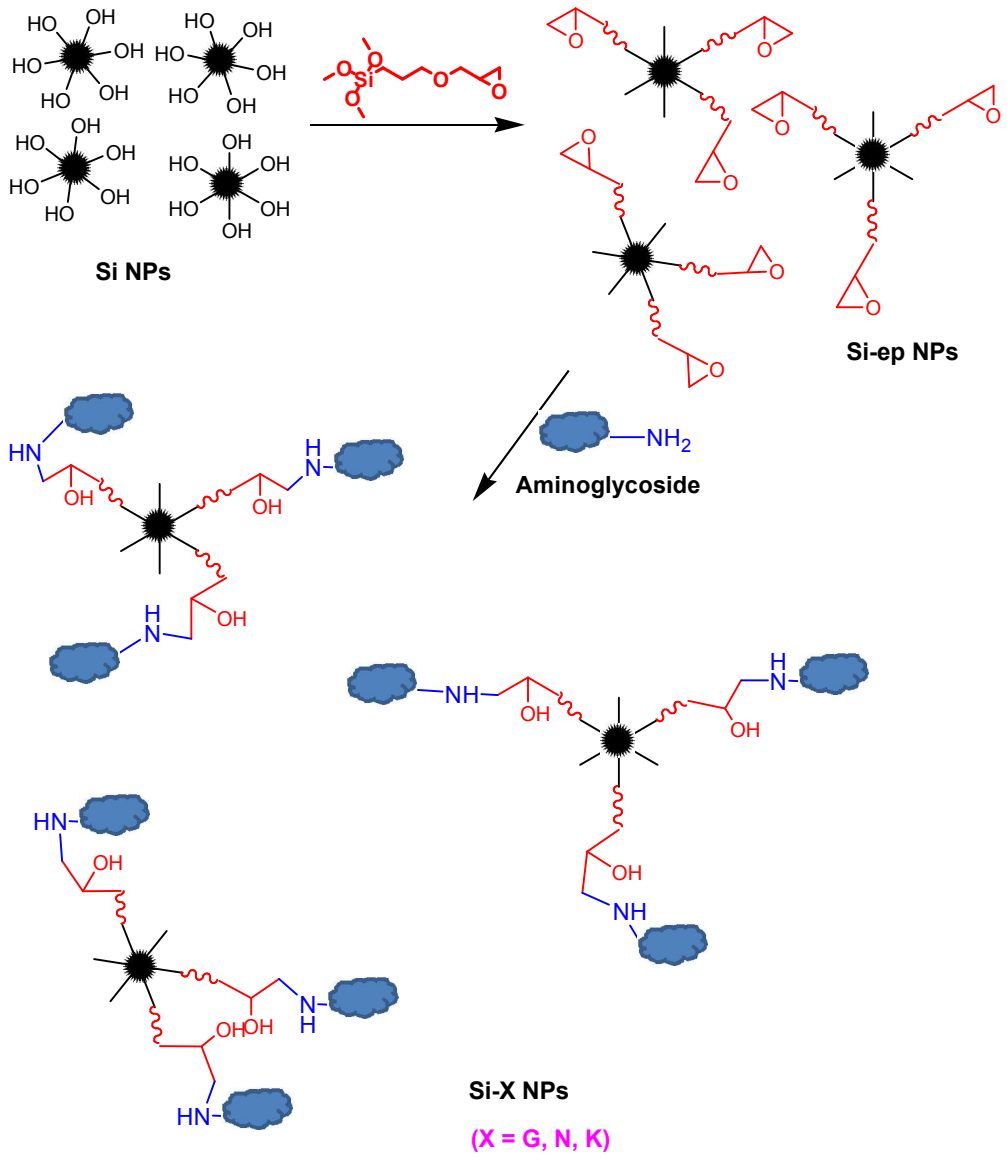

Scheme 1. Preparation of aminoglycoside-conjugated silica nanoparticles (Si-X NPs).

Table 1. Size (diameter) and zeta potential (surface charge) measurements of silica, epoxy silica and aminoglycoside-conjugated silica NPs

Nanoparticle samples	Size (d.nm) ± SD	Zeta potential (mV) ± SD
Native silica (Si-NPs)	160 ± 12.0	-41.4 ± 1.0
Si-ep	223 ± 17.0	-31.0 ± 0.6
S-G	256 ± 10.0	+34.1 ± 1.3
S-N	298 ± 14.0	+35.5 ± 2.0
S-K	269 ± 22.0	+24.1 ± 1.5

Both size and zeta potential measurements showed an almost regular pattern with respect to aminoglycosides. The physical size of the antibiotics almost dictated the size of the nanoparticles, i.e. structurally, among these aminoglycosides, neomycin, being the biggest one, generated bigger sized conjugate nanoparticles as compared to kanamycin- and gentamicin-Si NPs, which bear almost similar structures. These two produced conjugate nanoparticles in the range of 256-269 nm. Likewise, neomycin, having six primary amino groups, generated the particles of the highest positive charge. Gentamicin with five amines (4 primary and 1 secondary amines) displayed higher positive charged S-G nanoparticles as compared to kanamycin-functionalized silica nanoparticles, wherein the aminoglycoside consisted of only four primary amines. Further, transmission electron microscopy (TEM) was also used to show the morphology of the nanoparticles. Figure 1 shows TEM images of native silica and functionalized silica nanoparticles. These images show the spherical shaped particles, but aggregated in aqueous medium.

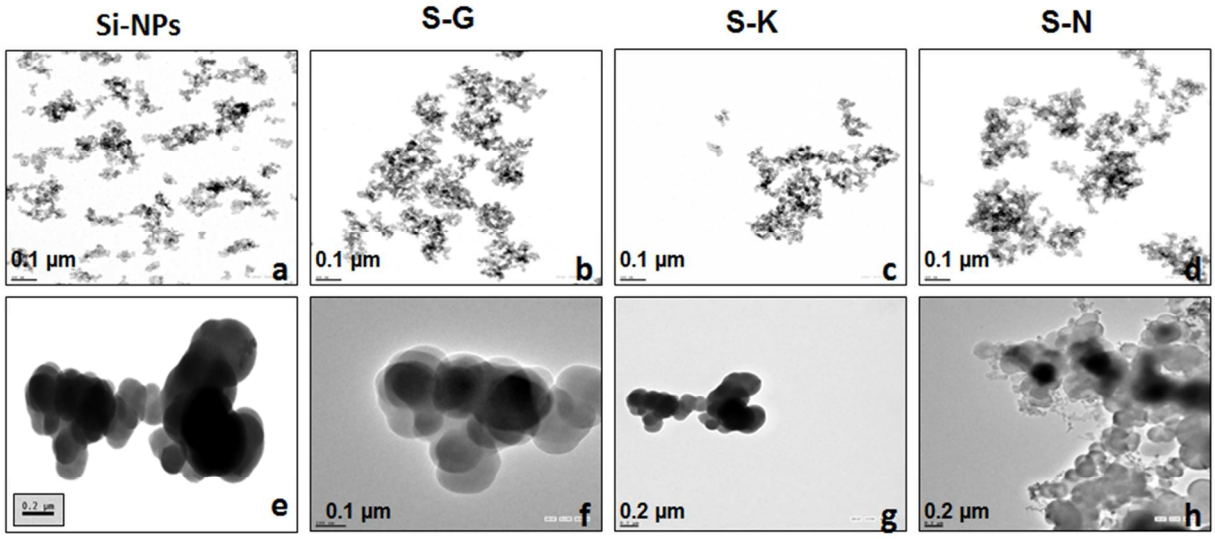

Figure 1. TEM images of native and aminoglycoside-conjugated silica nanoparticles. Scale bars in a-d, f = 0.1 µm and in e, g, h = 0.2 µm.

FTIR spectra of all the samples were recorded, however, no significant difference in the position of the stretching frequency of the functional groups was observed except in the intensity of the peaks. This might be due to the amorphous nature of silica nanoparticles. After conjugation, the peaks become more intense as shown in figure 2. A peak at 1170 cm^{-1} clearly indicated the presence of Si-O-Si bond which also merged with the C-O stretching peak (at 1200 cm^{-1}). Likewise, $-NH_2$ and –OH groups, both showed same stretching frequency, although differed in intensity (3300-3450 cm^{-1}). These results are in agreement with the previous ones reported in the literature.[38,39]

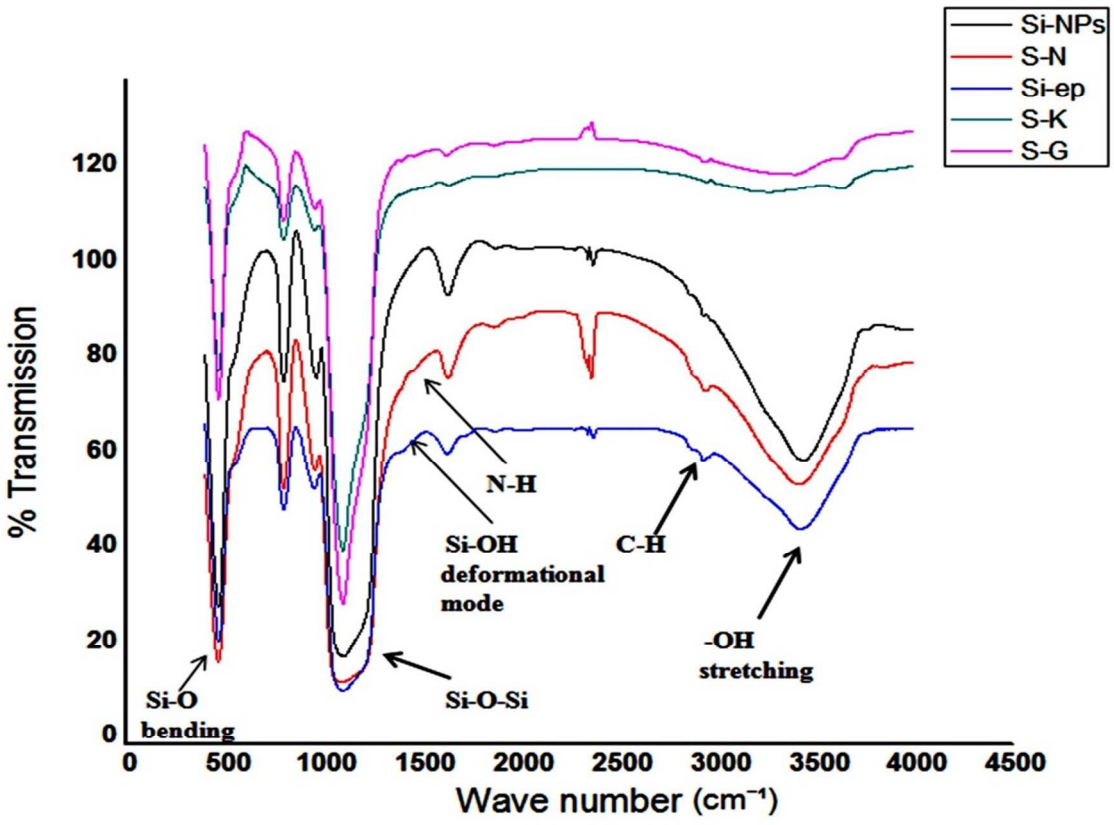

Figure 2. FTIR spectra of silica nanoparticles (Si NPs), epoxy-silica (Si-ep), silica-gentamicin (S-G), silica-neomycin (S-N) and silica-kanamycin (S-K) nanoparticles.

X-ray diffraction (XRD) analysis of native, activated and functionalized silica nanoparticles was also carried out. However, like FTIR results, here too, not much difference was observed in XRD graphs (Fig. S1, *see ESI*) indicating that the silica nanoparticles used in the study were amorphous in nature. Amorphous materials do not show clear peaks in their XRD spectra, as also reported in the literature.[39,40]

Thermogravimetric analysis (TGA) results of native, activated and functionalized silica nanoparticles are depicted in figure 3. The results clearly showed the covalent conjugation of aminoglycosides with silica nanoparticles via epoxy-amine chemistry. The initial weight loss at ~100 ^{o}C in all the samples could be attributed to the removal of moisture content adsorbed on the surface or pores of the nanoparticles. Further weight loss at ~400 ^{o}C in S-G, S-K and S-N NPs accounted for elimination of glycosidic moieties, while weight loss at ~575 ^{o}C in all the samples might be due to loss of alkyl linker (glycidyloxypropyl).

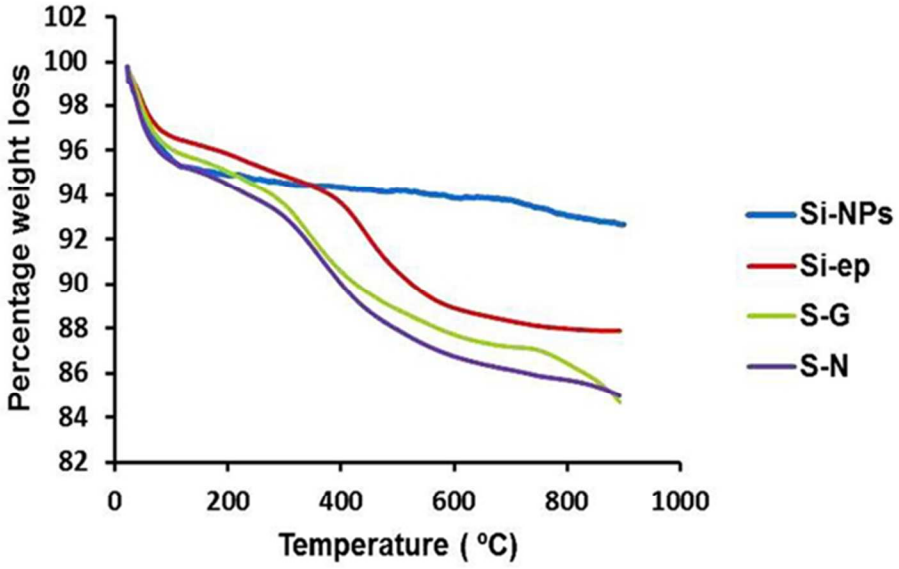

Figure 3. Thermogravimetric analysis of native (Si NPs), epoxy-silica nanoparticles (Si-ep) and aminoglycosides conjugated silica nanoparticles (silica-gentamicin, S-G and silica-neomycin, S-N). Percent weight loss was plotted against temperature (^{o}C). The weight loss ~400 ^{o}C was attributed to the decomposition of aminoglycosides.

Enhanced antibacterial activity of aminoglycoside-conjugated silica nanopaticles

In order to assess the antibacterial efficacy of the aminoglycoside-conjugated silica nanoparticles, the microbroth dilution assay was performed in 96-well plates as described previously.[41,42] Samples of aminoglycoside-conjugated silica nanoparticles were made in autoclaved Milli Q water at different concentrations (1, 2, 4 mg/ml). Bacteria (*BC, SA, EC and ST*) were incubated with different samples for different time intervals (0, 3, 6, 9, 12 and 15h). The wells showing pink to red color on addition of tetrazolium dye (INT) indicated bacterial growth while the wells remained colorless showed antimicrobial activity. The plots between OD (600 nm) and time (h) for various silica NPs (Fig. 4) displayed a considerable change in OD of the culture containing only silica NPs, which indicated an uncontrolled growth of bacteria, while the culture wells, containing aminoglycoside-conjugated silica NPs, showed a very small change in OD signifying very low or negligible growth.

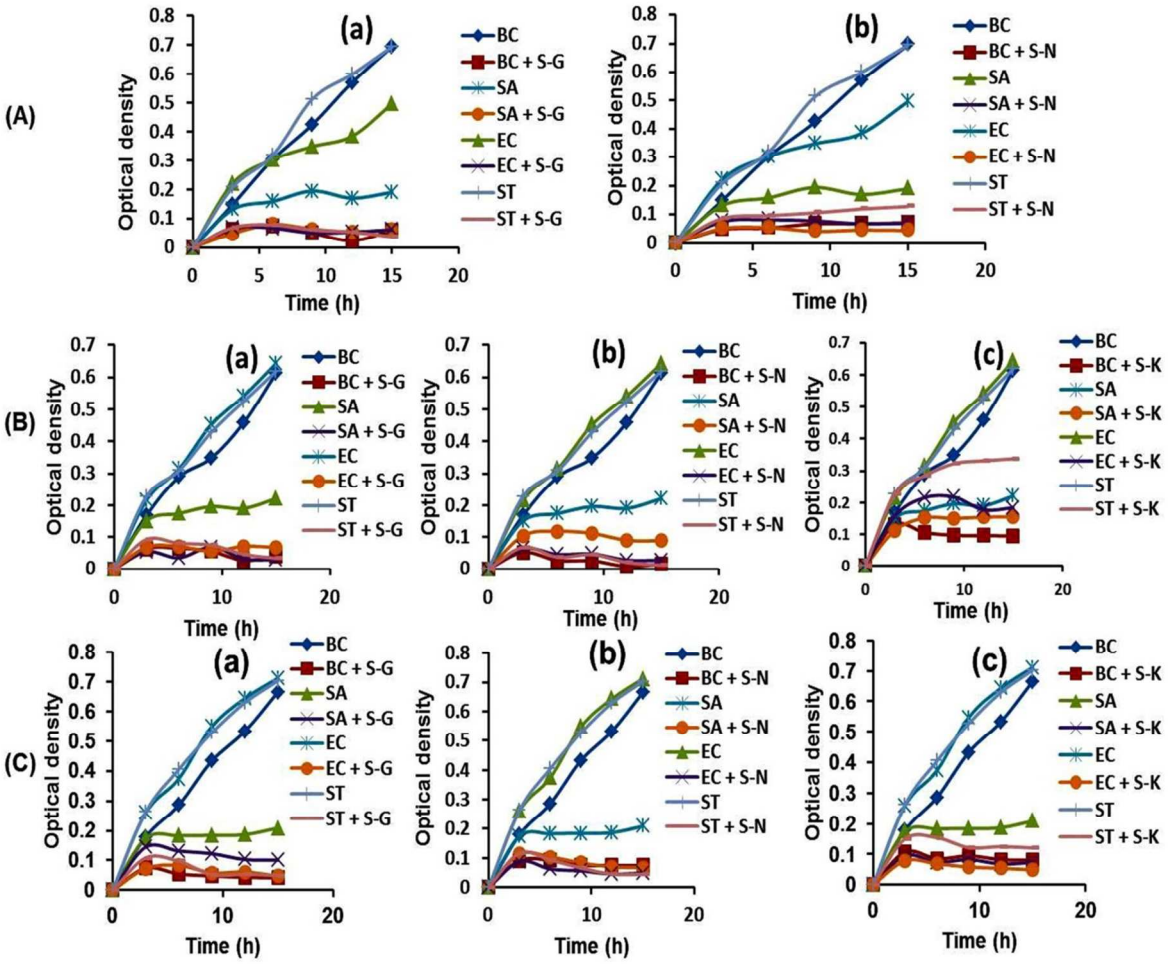

Figure 4. Growth curves of different bacteria [*Bacillus cereus (BC), Staphylococcus aureus (SA), Escherichia coli (EC)* and *Salmonella enteric typhimurium (ST)*] at various concentrations (A) 1 mg/ml, (B) 2 mg/ml, and (C) 4 mg/ml of native silica and aminoglycoside-conjugated silica nanoparticles [(a) silica-gentamicin, S-G; (b) silica-neomycin, S-N; (c) silica-kanamycin, S-K].

Determination of minimum inhibitory concentration of aminoglycoside-conjugated silica nanoparticles

Minimum inhibitory concentration (MIC), the lowest concentration of an antimicrobial agent that prevents the growth of the microorganism, of native and functionalized silica nanoparticles was determined to inhibit the growth of different Gram-positive and Gram-negative bacteria. Serially diluted sample solutions (0.8 – 0.005 mg/ml) were prepared, mixed with 10^5 CFU/ml and incubated overnight. The results are depicted in Table 2. In Gram-positive bacteria (*BC* and *SA*), the lowest MIC values were exhibited by S-G NPs, while in Gram-negative bacteria (*EC* and *ST*), S-G and S-N NPs showed the lowest MICs. S-K NPs displayed relatively higher MICs in both Gram-positive and Gram-negative bacteria. All the functionalized silica nanoparticles

showed considerably low MICs as compared to native silica NPs, however, these MICs were higher as compared to MICs exhibited by the native aminoglycosides. This reduced activity of the aminoglycoside-conjugated silica nanoparticles could be due to the conjugation of the aminoglycosides with activated silica NPs, wherein some of the primary amines got converted into secondary amines, which carried lower charge density as compared to primary ones. Hence, the reduction in charge density could be attributed to lower antimicrobial activity of the functionalized silica nanoparticles.

Table 2. Minimal Inhibitory Concentration (MIC) in μg/ml of aminoglycoside-conjugated silica nanoparticles in different bacterial strains and the values in parentheses are the standard MIC of the respective free aminoglycosides in μg/ml. MIC of native silica nanoparticles is in mg/ml.

Sample	*E. coli*	*S. typhimurium*	*B. cereus*	*S. aureus*
S-G	95 (4)	100 (1)	70 (0.1)	80 (0.1)
S-N	100 (8)	95 (0.1)	80 (0.1)	85(0.5)
S-K	400 (1)	420 (1)	380 (1)	360 (0.1)
Si-NPs (mg/ml)	>30	>30	>30	>30

Subsequently, the survival percentage of microbes (*EC, ST and BC, SA*) was determined using the functionalized silica nanoparticles (S-G, S-N and S-K NPs) post-6h of incubation at different concentrations. The results showed that these functionalized silica NPs were quite efficient in inhibiting the bacterial growth (Fig. 5). Hence, aminoglycoside-conjugated silica nanoparticles exhibited enhanced antimicrobial competency than the native silica and thus these can be considered as better antimicrobial drug alternatives in near future.

Non-toxic behaviour of aminoglycoside-conjugated silica nanoparticles

Cytotoxicity plays an important role in assessing the antimicrobial acivity of the cationic nanomaterials. To be useful for clinical applications, excellent activity against bacteria with minimal effect on mammalian cells is considered as one of the major requirements of an antimicrobial agent. Here, we have evaluated the cytotoxicity of the aminoglycoside-conjugated silica nanoparticles on erythrocytes as well as mammalian cells. Hemolysis assay, carried out upto 50x of MIC values, showed low toxicity of the functionalized silica nanoparticles, whereas the native silica NPs showed a concentration dependent high toxicity (Fig. 6). Similarly, cell viability assay was performed upto 10x MICs values on MCF-7 cells which revealed that aminoglycoside-conjugated silica nanoparticles (S-G and S-K) and aminoglycosides (G, N and K) displayed more than 80% cell viability at all the tested concentrations while S-N showed cell viability in the range of ~70-80 % and silica nanoparticles (Si-NPs), being toxic in nature at their higher concentration, exhibited cell vibility in the range of ~35-40 % (Fig.7).

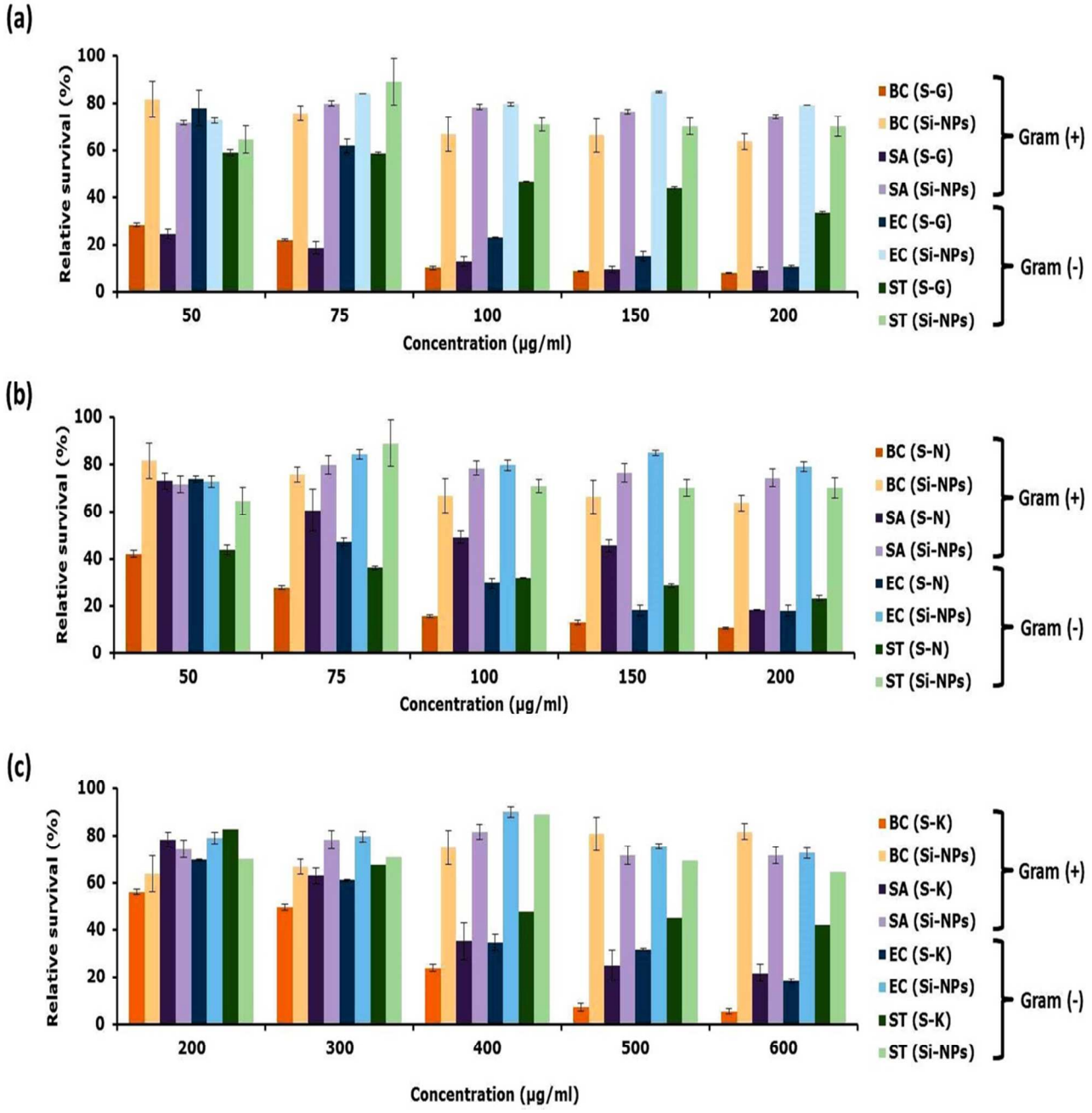

Figure 5. Relative survival (%) of bacterial strains (both Gram-positive and Gram-negative) treated with native and aminoglycoside-conjugated silica nanoparticles at different concentrations (µg/ml) for a period of 6h. (a) bacteria treated with native silica and S-G nanoparticles; (b) bacteria treated with native silica and S-N nanoparticles, and (c) bacteria treated with native silica and S-K nanoparticles.

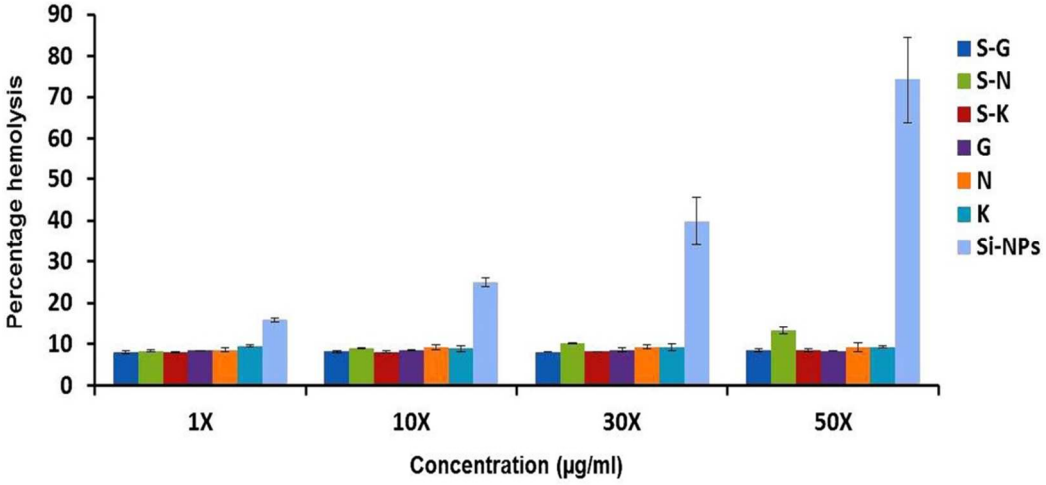

Figure 6. Hemolysis assay of silica-gentamicin (S-G), silica-neomycin (S-N), silica-kanamycin (S-K), native silica (Si-NPs) and free aminoglycosides at different multiples of MICs (µg/ml). Native silica nanoparticles (Si-NPs) were used at concentrations of 400, 4000, 12000 and 20000 µg/ml.

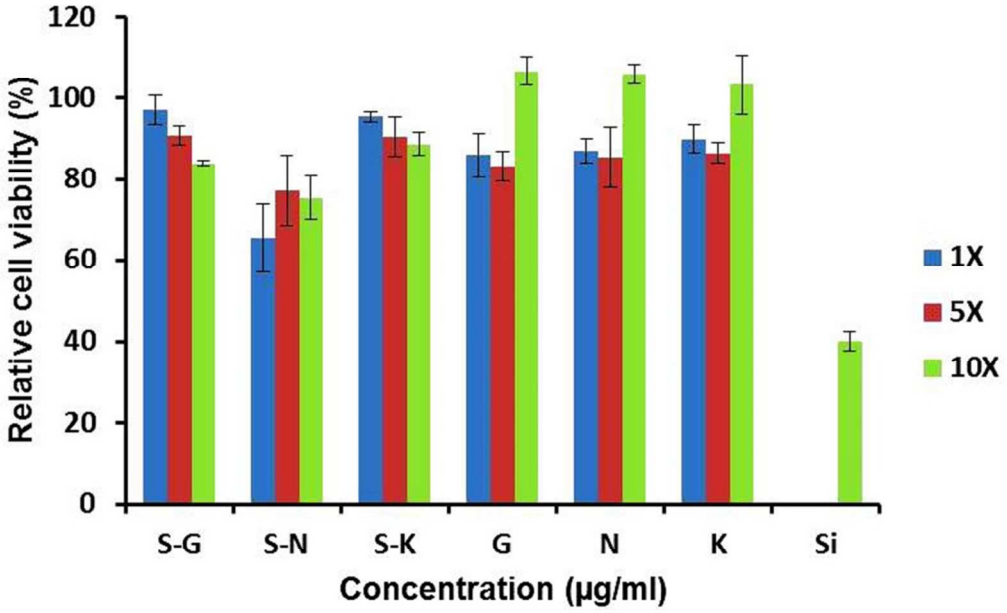

Figure 7. Cell viability assay of silica-gentamicin (S-G), silica-neomycin (S-N), silica-kanamycin (S-K), native silica (Si-NPs) and free aminoglycosides (G, N, K) at different multiples of MICs (µg/ml). Native silica nanoparticles (Si-NPs) were used at concentration of 4000 µg/ml (10x).

Bactericidal action of aminoglycoside-conjugated silica nanoparticles by TEM

In order to test the contact-killing mechanism of the functionalized silica nanoparticles at the microscopic level, we performed TEM using native silica as control. Bacterial colonies were incubated with native silica nanoparticles for 1h, while with functionalized silica nanoparticles, incubation was performed at two time points (15 and 30 min). Figure 8 illustrates the images of native bacteria (*BC*) (Fig. 8a), *BC* treated with silica (1h) and functionalized silica nanoparticles (15 min). Silica NPs treated bacteria did not show any morphological changes, i.e. silica NPs do not have any activity upto 1h of incubation (Fig. 8b), however, in case of S-G (Fig. 8c), S-K (Fig. 8d) and S-N (Fig. 8e) nanoparticles treated bacteria at 5x MIC, significant disruption in the cell wall of bacteria observed even after 15 min, while post-30 min, complete disintegration of bacteria occurred (Fig. S2, *see ESI*). These results ensure the potential of aminoglycoside-silica nanoparticles to be widely used as efficient antimicrobial agents for other types of microorganisms.

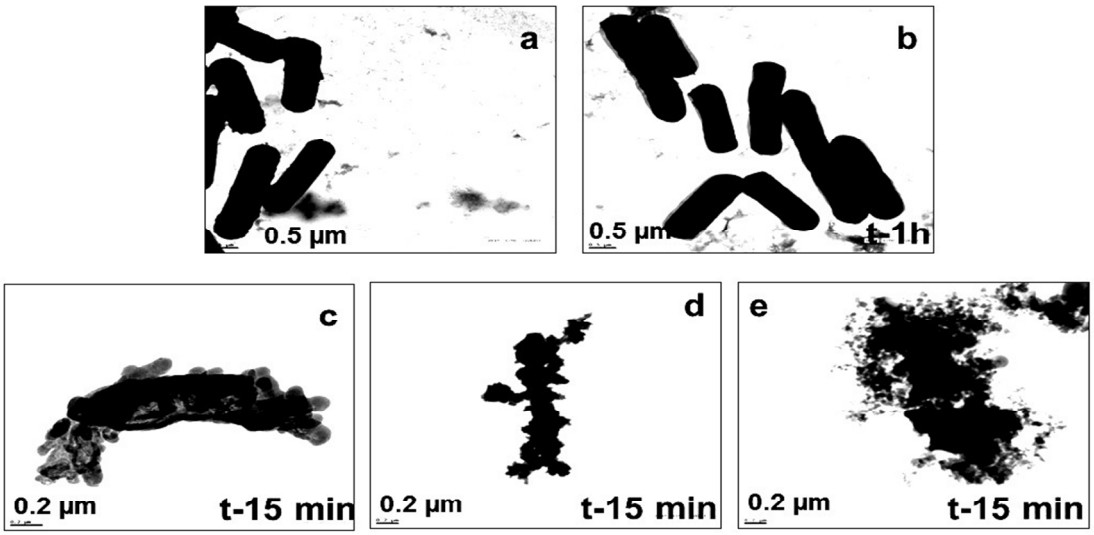

Figure 8. TEM images of *Bacillus cereus* (BC) (a) untreated, (b) treated with native silica nanoparticles (Si-NPs) at concentration of 2000 µg/ml (5x MIC) for 1 h, (c) treated with silica-gentamicin (S-G) at concentration of 350 µg/ml (5x MIC) for 15 min, (d) treated with silica-kanamycin (S-K) at concentration of 1900 µg/ml (5x MIC) for 15 min, and (e) treated with silica-neomycin (S-N) at concentration of 400 µg/ml (5x MIC) for 15 min.

Enhanced efficacy of silica-kanamycin nanoparticles against resistant strain

The above results established the antimicrobial efficacy of the functionalized silica

nanoparticles against known pathogens. These results prompted us to further examine their bactericidal activity against resistant bacterium. We treated kanamycin-resistant *E. coli* with kanamycin (upto 30x MIC) and S-K NPs (upto 10x MIC) for 12h. The results exhibited complete ineffectiveness of kanamycin on resistant *E. coli*, while S-K NPs were highly effective in concentration-dependent mode to show bactericidal effect (Fig. 9). At 10x MIC, there was ~42% higher killing as compared to free kanamycin. Higher MICs of S-K NPs could not be used because at higher concentrations, S-K NPs showed tendency to aggregate after 4-5h. Taken together, it was noteworthy that S-K NPs showed enhanced antibacterial activity even against kanamycin-resistant *E. coli*, which might be due to altered mechanism of action of these NPs.

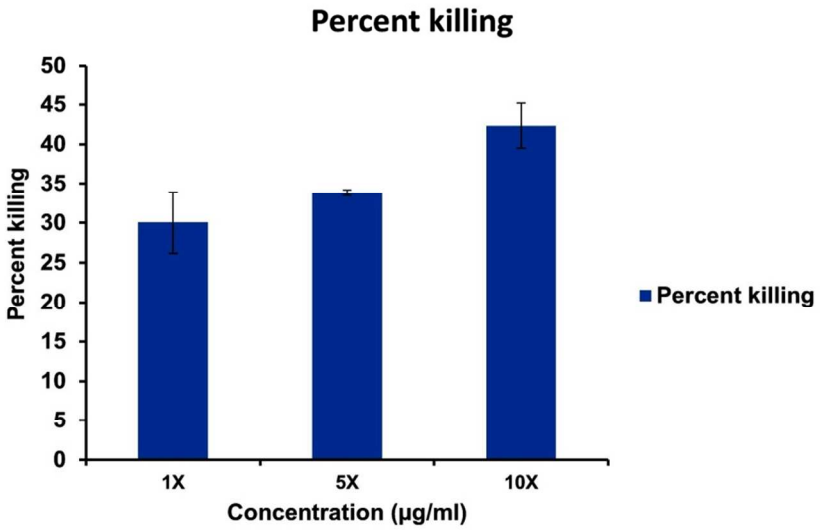

Figure 9. Enhanced percent killing of the resistant bacterial strain of *E. coli* at different concentration of minimum inhibitory concentration (MICs, µg/ml) of silica-kanamycin NPs in comparison to free kanamycin. MIC: 1x, 400 µg/ml; 5x, 2000 µg/ml; 10x, 4000 µg/ml.

Conclusions

In conclusion, we have demonstrated the excellent efficacy of nanomaterial-based antimicrobial agents against nosocomial as well as antibiotic-resistant bacteria. Though conjugation of aminoglycosides to silica nanoparticles, which are considered as efficient carriers of biomolecules *in vitro* and *in vivo*, decreased the activity compared to native aminoglycosides, however, exhibited excellent activity against resistant strain and maintained bactericidal activity without compromising on cytotoxicity. The strategy provides very facile and rapid functionalization of silica nanoparticles. We hope that the projected methodology would help in synthesizing conjugates of other antimicrobials to address multi-drug bacterial resistance, which is growing at much alarming pace. Further research in the direction to improve the aqueous dispersibility of the functionalized silica nanoparticles is under progress in the authors' laboratory.

Acknowledgements

Financial support from CSIR-network projects (BSC0120 and BSC0302) is gratefully acknowledged. The authors also thank University Science Instrumentation Centre, Delhi University, Delhi, to get these samples analyzed. SA and RP thank CSIR and UGC, New Delhi, respectively, for providing research fellowships to carry out the present work.

References

1 G. McDonnell and A. D. Russell, *Clin. Microbiol. Rev.,* 1999, 12, 147-179.

2 M. Simões, *Curr. Med. Chem.,* 2011, **18**, 2129-2145.

3 W. A. Rutala and D. J. Weber, *Clin. Infect. Dis.,* 2004, **39**, 702-709.

4 A. J. Alanis, *Arch. Med. Res.,* 2005, **36**, 697-705.

5 (a) G. D. Wright and A. D. Sutherland, *Trends Mol. Med.,* 2007, **13**, 260-267**;** (b) R. J. Fair and Y. Tor, *Perspect. Medicin. Chem.*, 2014, **6**, 25-64; (c) V. Hernandez, T. Crépin, A. Palencia, S. Cusack, T. Akama, S. J. Baker, W. Bu, L. Feng, Y. R. Freund, L. Liu, M. Meewan, M. Mohan, W. Mao, F. L. Rock, H. Sexton, A. Sheoran, Y. Zhang, Y. K. Zhang, Y. Zhou, J. A. Nieman, M. R. Anugula, E. M. Keramane, K. Savariraj, D. S. Reddy, R. Sharma, R. Subedi, R. Singh, A. O'Leary, N. L. Simon, P. L. De Marsh, S. Mushtaq, M. Warner, D. M. Livermore, M. R. K. Alley and J. J. Plattner, *Antimicrob. Agents Chem.*, 2013, **57**, 1394−1403.

6 S. Y. Sung, L. T. Sin, T. T. Tee, S. T. Bee, A.R. Rahmat, W.A.W.A. Rahman, A. C. Tan and M. Vikhraman, *Trends Food Sci. Technol.,* 2013, **33**, 110-123.

7 L. Gutierrez, A. Escudero, R. Battle and C. Nerin, *J. Agri. Food Chem.,* 2009, **57**, 8564-8571.

8 J. Y. Maillard, *Ther. Clin. Risk Manag.,* 2005, **1**, 307-320.

9 S. M. Lee, K. H. Liu, Y. Y. Liu, Y. P. Chang, C. C. Lin and Y. S. Chen, *Materials,* 2013, **6**, 1391-1402.

10 Z. Chen and Y. Sun, *Indus. Eng. Chem. Res.,* 2006, **45**, 2634-2640.

11 X. Sun, Z. Cao and Y. Sun, *Indus. Eng. Chem. Res.,* 2009, **48**, 607-612.

12 M. A. Kohanski, D. J. Dwyer, B. Hayete, C. A. Lawrence and J. J. Collins, *Cell,* 2007, **130**, 797-810.

13 A. D. Fuchs and J. C. Tiller, *Angew. Chem. Int. Ed.,* 2006, **45**, 6759-6762.

14 M. Tischer, G. Pradel, K. Ohlsen and U. Holzgrabe, *ChemMedChem,* 2012, **7**, 22-31.

15 S. Lenoir, C. Pagnoulle, M. Galleni, P. Compere, R. Jerome and C. Detrembleur, *Biomacromolecules,* 2006, **7**, 2291-2296.

16 A. Alamri, M. H. El-Newehy and S. S. Al-Deyab, *Chem. Cent. J.,* 2012, **6**, 111.

17 A. M. Carmona-Ribeiro and L. D. de Melo Carrasco, *Int. J. Mol. Sci.,* 2013, **14**, 9906-9946.

18 A. Peschel and H. G. Sahl, *Nat. Rev. Microbiol.,* 2006, **4**, 529-536.

19 M. Millard, D. Pathania, Y. Shabaik, L. Taheri, J. Deng and N. Neamati, *Plos One,* 2010, **5**, e13131.

20 D. D. Iarikov, M. Kargar, A. Sahari, L. Russel, K. T. Gause, B. Behkam and W. A. Ducker, *Biomacromolecules,* 2014, **15**, 169-176.

21 (a) F. Tang, L. Li and D. Chen, *Adv. Mater.,* 2012, **24**, 1504-1534; (b) S. M. Dizaj, S. Jafari and A. Y. Khosroushahi, *Nanoscale Res. Lett.*, 2014, **9**, 252; (c) S. S. Jun, B. Xia and L.S. Bok, *Drug Discov. Today*, 2007, **12**, 650–656; (d) Z. P. Xu, Q. H. Zeng, G. Q. Lu and A. B. Yu, *Chem. Eng. Sci.*, 2006, **61**, 1027–1040.

22 C. Hom, J. Lu and F. Tamanoi, *J. Mater. Chem.,* 2009, **19**, 6308-6316.

23 Z. Li, J. C. Barnes, A. Bosoy, J. F. Stoddart and J. I. Zink, *Chem. Soc. Rev.,* 2012, **41**, 2590-2605.

24 M. Montalti, L. Prodi, E. Rampazzo and N. Zaccheroni, *Chem. Soc. Rev.,* 2014, **43**, 4243-4268.

25 U. Jeong, Y. Wang, M. Ibisate and Y. Xia, *Adv. Funct. Mater.,* 2005, **15**, 1907-1921.

26 N. Singh, A. Karambelkar, L. Gu, K. Lin, J. Miller, C. Chen, M. Sailor and S. Bhatia, *J. Am. Chem. Soc.,* 2011, **133**, 19582-19585.

27 R. Xing, H. Lin, P. Jiang and F. Qu, *Coll. Surf. A: Physicochem. Eng. Aspects,* 2012, **403**, 7-14.

28 F. Y. Qu, G. S. Zhu, S. Y. Huang, S. G. Li and S. L. Qiu, *ChemPhysChem,* 2006, **7**, 400-406.

29 A. Dong, Q. Zhang, T. Wang, W. Wang, F. Liu and G. Gao, *J. Phys. Chem. C,* 2010, **114**, 17298-17303.

30 J. Song, H. Song, H. Kong, J. Y. Hong and J. Jang, *J. Mater. Chem.,* 2011, **21**, 19317-19323.

31 A. Dong, J. Huang, S. Lan, T. Wang, L. Ziao, W. Wang, T. Zhao, X. Zheng, F. Liu, G. Gao and Y. Chen, *Nanotechnology,* 2011, **22**, 295602.

32 L. Djouhri-Bouktab, J. M. Rolain and J. M. Brunel, *Anti-infect. Agents,* 2014, **12**, 95-103.

33 T. F. Mika and R. S. Bauer, in Epoxy resins: Chemistry and technology. 2nd Ed. CRC Press, California, USA; 1988, pp. 465-550.

34 L. S. Gonzalez III and J. P. Spencer, *Am. Fam. Physician*, 1998, **58**, 1811-1820.

35 F. Baquero, *J. Antimicrob. Chemother.*, 1997, **39**, 1-6.

36 S. Bardal, J. Waechter and D. Martin, in Applied Pharmacology, Chapter 18: Infectious Diseases. Elsevier Health Science, NY; 2011, pp. 233-291.

37 G. T. Hermanson, in Bioconjugate techniques. Academic Press, UK; 2008.

38 B. Sahoo, K. Sanjana P. Devi, S. K. Sahu, S. Nayak, T. K. Maiti, D. Dhara and P. Pramanik, *Biomater. Sci.,* 2013, **1**, 647-657.

39 R. B. Kozakevych, Y. M. Bolbukh and V. A. Tertykh, *World J. Nanosci. Eng.,* 2013, **3**, 69-78.

40 T. López, J. L. Bata-García, D. Esquivel, E. Ortiz-Islas, R. Gonzalez, J. Ascencio, P. Quintana, G. Oskam, F. J. Álvarez-Cervera, F. J. Heredia-López and J. L. Góngora-Alfaro, *Int. J. Nanomed.,* 2011, **6**, 19-31.

41 R. Bansal, R. Pathak, D. Jha, P. Kumar and H. K. Gautam, *Int. J. Polym. Mater. Polym. Biomater.,* 2015, **64**, 84-89.

42 S. Yadav, M. Mahato, R. Pathak, D. Jha, B. Kumar, S. R. Deka, H. K. Gautam and A. K. Sharma, *J. Mater. Chem. B,* 2014, **2**, 4848-4861.